Journal of Simulation and Analysis of Novel Technologies in Mechanical Engineering
17 (1) (2025) 0053~0066
DOI 10.71939/jsme.2025.1207115

Research article

Numerical simulation and comparison of hepatic tumor hyperthermia using microwave and radiofrequency waves

Hamoon Pourmirzaagha*, Parimah Salimi

Department of Mechanical and Aerospace Engineering, Ram.C., Islamic Azad University, Ramsar, Iran

*Hamoon.pourmirzaagha@iau.ac.ir

(Manuscript Received --- 17 May 2025; Revised --- 13 July 2025; Accepted --- 01 Aug. 2025)

Abstract

In this study, the thermal ablation of liver tumors using radiofrequency (RF) and microwave (MW) energy was numerically investigated. Heat transfer within the tissue was simulated based on coupled electromagnetic and bioheat models, employing a realistic liver geometry in COMSOL Multiphysics. Unlike previous studies that primarily used simplified cylindrical models, this work utilized actual tissue structure to achieve a more accurate analysis of temperature distribution, electromagnetic field intensity, and the extent of necrosis. The results indicate that the highest degree of tumor cell destruction occurs in regions closest to the applicator, while both field intensity and temperature gradually decrease with distance, leading to reduced necrosis. The realistic model demonstrated greater accuracy in predicting local temperatures and thermal effects compared to simplified models. Based on the findings, to minimize unintended damage to surrounding healthy tissue, it is recommended to reduce the applied power (to 5 W for MW) and voltage (to 17 V for RF). These results can contribute to the optimization of non-invasive liver cancer treatments and the safer design of hyperthermia devices.

Keywords: Liver, Tumors, Radiofrequency, Microwave.

1- Introduction

Cancer remains a major global health concern and stands as the second most common cause of death, following cardiovascular conditions [1]. It originates from abnormal and uncontrolled cell changes that eventually lead to the development of tumors [2]. Tumors are generally classified into benign and malignant types. Malignant tumors have the ability to invade surrounding tissues and spread to other parts of the body through the bloodstream or lymphatic system—a process known as metastasis. This progression complicates cancer treatment and increases resistance to conventional therapies. Early-stage cancer is more effectively treated, often through surgical interventions complemented by chemotherapy or radiotherapy. However, in advanced stages, treatment mainly aims to control the disease or slow its progression. Addressing cancer in its early phases, when metastasis has not yet occurred, significantly improves treatment outcomes [3].

Numerous studies have shown that preventing or detecting metastasis at early stages can greatly reduce cancer-related mortality. Emerging therapeutic approaches such as immunotherapy and targeted therapies, which attack specific cancer cells and molecular pathways, have introduced new hope for patients with advanced-stage cancer. While primary tumors can often be managed through surgery or chemotherapy, metastatic tumors typically exhibit resistance to treatment [4]. Cancer treatment modalities vary widely and may include surgery, chemotherapy, radiotherapy, photodynamic therapy, immunotherapy, gene therapy, and anti-angiogenic strategies. Selecting an appropriate method that ensures complete tumor ablation with minimal damage to healthy tissue is crucial. One promising method is hyperthermia therapy, in which tumor tissues are exposed to elevated temperatures to destroy malignant cells. Hyperthermia is widely used in treating tumors of internal organs such as the liver, kidneys, lungs, and bones. Cancer cells are thermally sensitive; exposure to temperatures between 41°C and 46°C for 20–60 minutes can inhibit their proliferation [5, 6]. Tumor cell death can occur via necrosis, an acute process resulting in visible tissue damage, or apoptosis, a gradual, programmed cell death that allows cellular debris to be cleared without major tissue disruption. Both types of cell death are induced during hyperthermia therapy. Techniques such as microwave or monopolar radiofrequency energy can directly induce necrosis at the treatment site, while apoptosis tends to occur in adjacent tissues.

Various energy sources including radiofrequency, microwave, high-intensity focused ultrasound (HIFU), and lasers are employed in hyperthermia. With the help of ultrasound or CT imaging, the precise location of the tumor is determined for targeted thermal application.

Microwave and radiofrequency (RF) hyperthermia have a prominent role in treating liver tumors due to their significant tissue penetration depth, ability to deliver focused energy to deep-seated tissues, and relatively easier temperature control within the targeted area. In contrast, laser hyperthermia offers high spatial precision, enabling accurate targeting of small lesions; however, its limited penetration depth confines its use primarily to superficial or moderately deep tumors and requires sophisticated and costly optical systems. Focused ultrasound hyperthermia can noninvasively transmit energy to deep tissues but demands precise adjustment of physical parameters and real-time imaging guidance for effective energy delivery. The optimal selection of hyperthermia modality depends on tumor location, size, and type, as well as available equipment and patient condition. Nonetheless, microwave and RF methods remain promising, controllable, and minimally invasive options for liver tumor treatment [7–11].

In radiofrequency hyperthermia, electrical currents in the range of 300 kHz to 1 MHz are used to deliver energy to target tissues. Frequencies between 450–500 kHz are typically employed for therapeutic purposes [12, 13]. This method relies on Joule heating, where current passing through conductive tissue generates heat [14]. Imaging techniques such as ultrasound, CT, or MRI guide electrode placement into the tumor. High-frequency electrical currents generate localized heat near the electrodes, effectively destroying cancer cells. While this method efficiently delivers energy to tissue, heat propagation

is limited by electrode reach and current strength, restricting the volume of treated tissue. Therefore, radiofrequency hyperthermia may be less effective for tumors near large blood vessels or those that have metastasized [13].

Microwaves, part of the electromagnetic spectrum, span frequencies from 300 MHz to 30 GHz. As they pass through polar molecule-rich tissues, these molecules oscillate in response to the electric field, generating heat through molecular collisions. Highly polar molecules respond more effectively to the electric field and heat up more rapidly. Additionally, charged ions in the tissue respond to the microwave field, increasing their motion and further contributing to heat production [15].

Microwave-based localized heating using microwave antennas was first developed in the 1970s and gained widespread medical use in the late 1980s [15, 16]. The advantages of microwave hyperthermia include its effectiveness in treating large tumors, tumors near major vessels, and even multiple tumors simultaneously. Although this method offers a higher treatment rate than radiofrequency ablation, it faces challenges in ensuring uniform energy absorption by tumors versus healthy tissues.

In recent years, significant research has focused on optimizing hyperthermia techniques and understanding their side effects [17–20]. Lu et al. [21] investigated how hepatic vessel diameter affects thermal injury during radiofrequency ablation. Their findings revealed that larger vessels (>4 mm in diameter) dissipate heat and protect surrounding tissues from thermal damage. In another study, numerical simulations using finite element methods were employed to evaluate the thermal sink effects of blood vessels during microwave ablation [22]. It was shown that the presence of vessels reduces peak temperature and that increased blood flow amplifies the heat sink effect. Ring et al. [23] found in experimental setups that the distance between vessels and the heat source, along with blood flow intensity, directly influences the heat sink phenomenon during microwave hyperthermia. Ma et al. [24] demonstrated that, in bipolar radiofrequency therapy, a blood flow rate of at least 10 mm/min is required for the heat sink effect to become significant.

Microwave ablation is recognized as a minimally invasive and fast-recovery method for destroying cancer cells using heat generated by microwave energy. Despite the clear advantages of this method, the interaction of the microwave probe with tissue can cause localized heating and damage to the surrounding tissues [25]. In another study, microwave thermal ablation was numerically modeled using finite element and finite volume methods to investigate its effects in a realistic human liver model. Different input powers and internal coolant flow rates of the probe were examined to predict tissue damage, and the simulated temperature results matched experimental data with less than 6% difference. This approach provides a reliable and repeatable framework for better understanding the effects of microwave ablation [26]. Liu et al. [27] focused on precise modeling of temperature distribution during microwave ablation of lung tumors using personalized parameters and finite element analysis. Their research contributed to improving treatment efficacy evaluation and optimizing microwave parameters. The results highlight the importance of accurate

modeling for enhancing the precision and effectiveness of the therapy.

Previous simulation studies have mostly used simplified geometries such as cylindrical models to analyze thermal and magnetic field behaviors in liver tissue. While these models simplify calculations, they fail to accurately capture the influence of real liver anatomy on temperature distribution, magnetic fields, and heat transfer processes.

In this study, for the first time, realistic 2D and 3D liver models were implemented in COMSOL software instead of cylindrical approximations. This geometrical shift allows for more accurate and realistic analysis of temperature profiles, thermal gradients, and magnetic field effects within hepatic tissue. The findings of this research may serve as a foundation for optimizing hyperthermia treatments and improving the effectiveness of non-invasive therapies for liver cancer.

A deeper understanding of energy distribution within biological tissues enables better tuning of treatment parameters to maximize cancer cell destruction while minimizing damage to healthy tissues—an essential aspect of personalized medicine for liver cancer patients. The results of this study may inform the design of advanced devices, enhance thermal targeting accuracy, and improve the overall efficiency of hyperthermia therapy. Consequently, treatment precision can be increased, side effects reduced, and therapeutic success rates improved—ultimately leading to better patient outcomes and quality of life.

2- Geometry of the Study

Figs. 1 and 2 illustrate the geometry and mesh grid of the liver model used in the numerical simulations. A three-dimensional (3D) geometry was implemented for radiofrequency (RF) heating to accurately resolve the electric and thermal field distributions. In contrast, a two-dimensional model was used for microwave (MW) heating, leveraging the symmetry of the applicator to reduce computational complexity.

For RF heating, voltages of 17 V and 22 V were applied over a period of 10 minutes, representing clinically relevant settings. MW heating simulations were performed at a frequency of 2.45 GHz, with input powers of 5 W and 10 W. These conditions allowed for direct comparison of the thermal response and ablation zones between the two techniques.

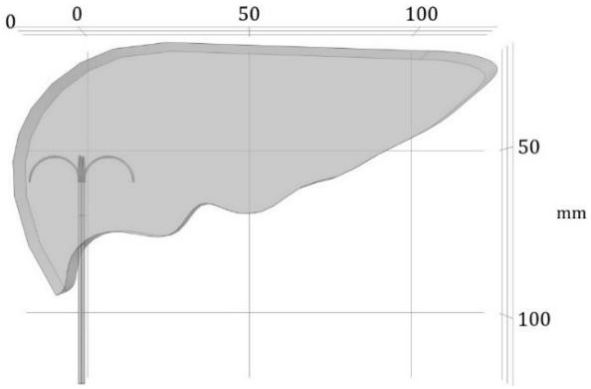

(a)

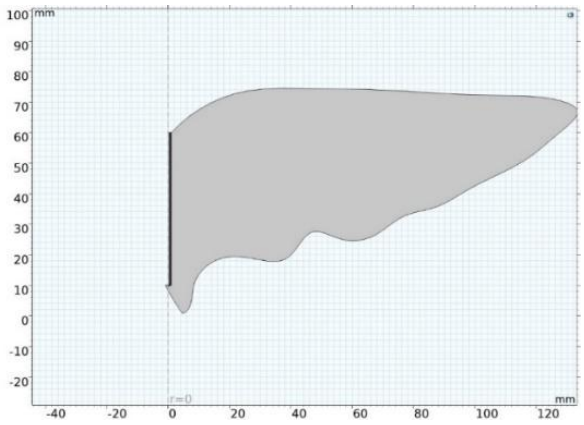

(b)

Fig. 1 Physical model used for the simulation of (a) radiofrequency heating and (b) microwave heating.

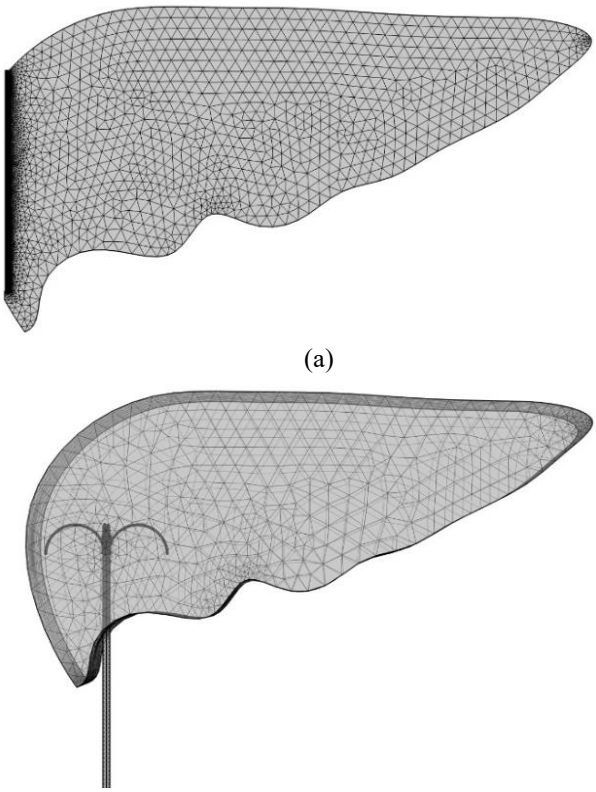

(a)

(b)

Fig. 2 Mesh grid for the simulation of (a) microwave heating and (b) radiofrequency heating.

3- Governing Equations

The most important parameter in evaluating the effectiveness of a hyperthermia method is the modeling of heat transfer and the determination of temperature changes in the target tissue. The tissue can be treated as a saturated porous medium. The most common and widely accepted model for this process is the Pennes bioheat transfer model [28].

$$\rho C_p \frac{\partial T}{\partial t} + \nabla.(k\nabla T) = \rho_b C_b W_b (T_b - T) + Q_{met} + Q_{ext} \quad (1)$$

In Equation (1), T is the local tissue temperature, T_b is the arterial blood temperature, C_b is the specific heat of blood, Q_{ext} denotes the external heat source, C_p is the specific heat of tissue, K is the thermal conductivity, w_b is the blood perfusion rate, and Q_{met} is the metabolic heat generation rate. The extent of tissue damage is calculated using the Arrhenius equation as follows [29]:

$$\frac{d\alpha}{dt} = A.\exp(-\frac{dE}{RT}) \quad (2)$$

In Equation (2), A is the frequency factor, dE represents the activation energy for irreversible tissue damage, and a is the damage function. These parameters are tissue-dependent. The ratio of damaged tissue volume to the total tissue volume is given by the following equation [29]:

$$\theta_d = 1 - \exp - \alpha \quad (3)$$

The propagation of electromagnetic waves in coaxial antennas is characterized by specific transverse electromagnetic (TEM) fields [29].

$$E = e_r \frac{C}{r} e^{i(\omega t - kz)} \quad (4)$$

$$H = e_\varphi \frac{C}{rz} e^{i(\omega t - kz)} \quad (5)$$

$$P_{av} = \int_{r_{inner}}^{r_{outer}} \mathrm{Re}(\frac{1}{2} E \times H^*) 2\pi r dr = e_z \pi \frac{c^2}{z} \ln(\frac{r_{outer}}{r_{inner}}) \quad (6)$$

In equations 4, 5, and 6, P_{av} represents the average power flow time at the antenna, Z is the wave impedance in the antenna's dielectric, and r_{innerr} and r_{outerr} are the inner and outer radii of the dielectric,

$$k = \frac{2\pi}{\lambda} \quad 7$$

In equation 7, λ represents the wavelength. To model the microwave antenna, the following equation has been used, where:

- ε_r : relative permittivity or dielectric constant
- ε_0 : vacuum permittivity constant (8.85×10^{-12} F/m)
- ω : angular frequency, (Rad/s)
- σ : electrical conductivity (S/m)
- μ_r : relative permeability

- H : magnetic field intensity, (A/m)
- k_0 : vacuum wave number

This equation is employed to accurately model the characteristics of the microwave antenna and its behavior under various electromagnetic field conditions.

$$\nabla\times\left((\varepsilon_r-\frac{i\sigma}{\omega\varepsilon_o})^{-1}\nabla\times H_\varphi\right)-\mu_r k_o^2 H_\varphi=0 \quad (8)$$

The feed point is defined as a port according to the following equation [29]:

$$n\times\sqrt{\varepsilon}E-\sqrt{\mu}H_\varphi=-2\sqrt{\mu}H_{\varphi 0} \quad (9)$$

$$H_{\varphi 0}=\frac{\sqrt{\dfrac{P_{av}z}{\pi r\ln\left(\dfrac{r_{outer}}{r_{inner}}\right)}}}{r} \quad (10)$$

When microwave energy is applied, the external heat source corresponds to the resistive heating generated by the electromagnetic field, which is given by Equation (11) [29]:

$$Q_{ext}=\frac{1}{2}\mathrm{Re}\left[(\sigma-j\omega\varepsilon)E.E^*\right] \quad (11)$$

The following equation corresponds to the electric current equation when using radio frequency. In this equation, v is the potential (in volts), σ is the electrical conductivity (S/m), J^e is the current density (A/m^2), and Q_j is the current source (A/m^3). In this model, both J^e and Q_j are zero [29].

$$-\nabla\cdot(\sigma\nabla V-J^e)=Q_i \quad (12)$$

4- Solution Method

To simulate radiofrequency heating, the bioheat transfer equation (Pennes equation) was solved concurrently with the electric current equation. For microwave heating, the bioheat transfer equation was coupled with the electromagnetic wave propagation equations based on Maxwell's equations. The modeling was performed in a fully coupled and simultaneous manner, encompassing the bioheat transfer equations, electric current equations (for RF waves), and electromagnetic wave propagation equations (for microwave waves). Detailed modeling aspects are as follows:

- The Pennes bioheat equation was employed to model heat transfer within biological tissue, accounting for thermal conductivity, blood perfusion rate, metabolic heat generation, and external heat sources.
- Microwave propagation was simulated by solving Maxwell's equations in a two-dimensional domain, utilizing a coaxial antenna model, assuming a homogeneous dielectric medium with constant physical properties.
- The electric current model for RF waves was implemented in three dimensions using the actual geometry of liver tissue, assuming constant electrical conductivity and perfect electrode-tissue contact.
- Tissue damage was evaluated based on the Arrhenius equation, with parameters chosen according to the characteristics of liver tissue under fixed assumptions.

This coupled multi-physics modeling approach provides an accurate representation of the thermal and electromagnetic phenomena occurring during hyperthermia treatment.

All computational simulations were executed on a 64-bit Windows 11 Pro system with an Intel Core i7 processor and 16 GB of RAM. The average runtime per simulation was approximately 10 minutes for the radiofrequency model and about 1 minute for the microwave model.

The physical properties of the biological tissues used in the microwave simulations are listed in Table 1, while those corresponding to the RF simulations are provided in Table 2.

Table 1: Physical properties of materials used in microwave heating simulations [30-33]

Material properties of components	$\sigma(\frac{s}{m})$	$k_r^{'}$	ε_r
Liver	1.69	1	43.03
Blood	0.667	1	1
Catheter	0	1	2.6
Dielectric material	0	1	2.03

Table 2: Physical properties of materials used in radiofrequency heating simulations [30-33]

Material properties of components	σ $(\frac{s}{m})$	K $(\frac{W}{m.k})$	C_p $(\frac{J}{kg.k})$	ρ $(\frac{kg}{m^3})$
Liver	0.33	0.51	3540	1079
Blood	0.667	0.543	4180	1000
Electrode	10^9	18	840	6450
Body	10^7	71	132	21500
Base	10^{-4}	0.026	1045	70

4-1- Boundary Conditions

The initial temperature of the tissue was assumed to be equal to the normal body temperature (37°C).

Microwave (MW) Model: Scattering boundary conditions were applied at the outer edges to simulate electromagnetic wave absorption and minimize reflections. An input port was also defined to deliver power to the antenna.

Radiofrequency (RF) Model: A specified electric potential (17 or 22 V) was applied to the active electrode, while ground conditions were imposed on the distant boundaries.

Tissue Homogeneity: The liver tissue was considered homogeneous for the purposes of simulation, although real tissue may contain in homogeneities such as blood vessels or fatty regions.

5- Results and Discussion

Figs. 3 and 4 show the temperature distribution and tissue necrosis levels in the case where hyperthermia is applied using radio frequency waves. As observed in these figures, with increasing distance from the heat source (electrode), the tissue temperature gradually decreases, and consequently, the level of necrosis also reduces. The highest level of tissue damage occurs in the region where the electrode is directly located. In this area, the tissue temperature reaches the necrosis threshold, and complete cellular destruction occurs. In adjacent regions, due to the gradual decrease in the intensity of the electromagnetic field and heat, only partial or moderate necrosis is observed. This pattern is a result of the physical behavior of heat distribution in biological environments. RF waves generate resistive heat through the creation of electric currents in the tissue. This heat is maximal near the electrode, and as the distance increases, the heating intensity decreases due to absorption and scattering of energy within the tissue. Therefore, the greatest heat transfer and thermal tissue destruction occur near the electrode, and this effect exponentially decreases as the distance from the energy application center increases.

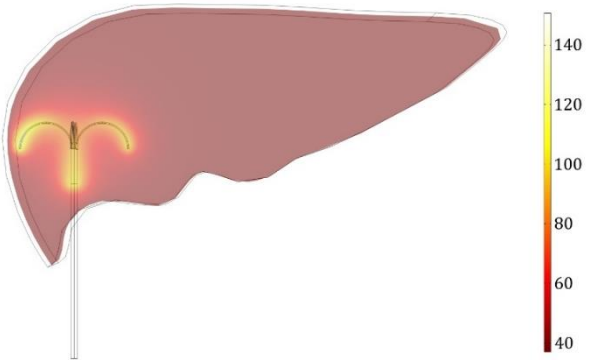

Fig. 3 Temperature contour in radiofrequency hyperthermia.

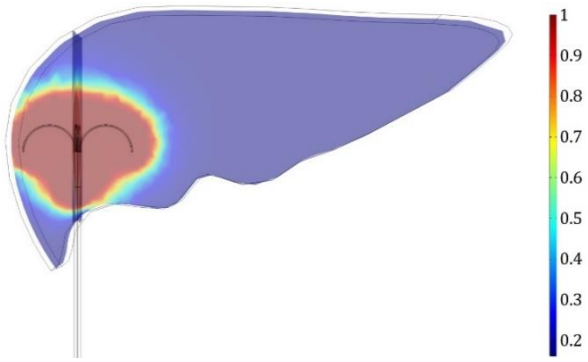

Fig. 4 Tissue necrosis contour in radiofrequency hyperthermia.

Figs. 5 and 6 illustrate the temperature distribution and tissue necrosis levels under conditions where hyperthermia treatment using microwave radiation has been applied. As shown in these graphs, the tissue temperature decreases with increasing distance from the heat source, and consequently, the level of necrosis also decreases.

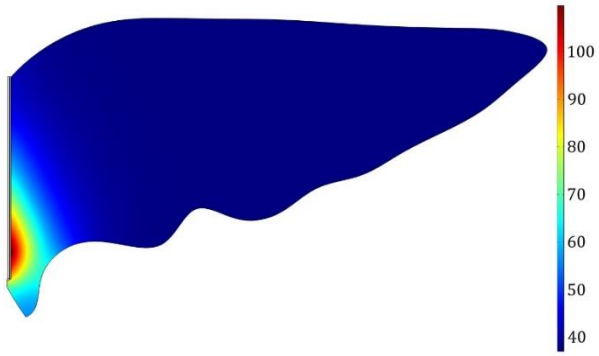

Fig. 5 Temperature contour in microwave hyperthermia.

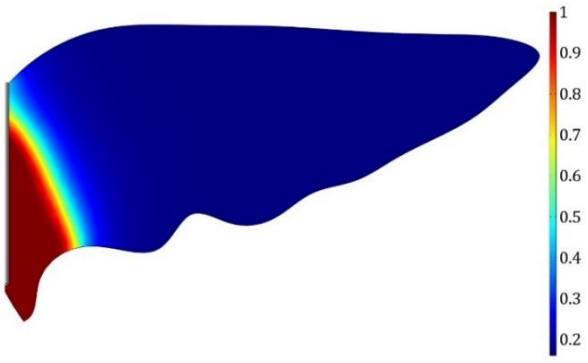

Fig. 6 Tissue necrosis contour in microwave hyperthermia.

This trend indicates a direct dependence of tissue damage intensity on the amount of energy absorbed in various regions. Microwaves are a form of high-frequency electromagnetic energy capable of inducing vibration in polar molecules, such as water. These vibrations cause molecular friction, ultimately generating localized heat within the tissue. The concentration of thermal energy is higher in regions close to the antenna or applicator, and as the distance increases, the energy of the waves diminishes due to absorption, attenuation, and scattering phenomena within the biological environment. As a result, the temperature generated in areas farther from the heat source is lower, and the extent of tissue necrosis decreases accordingly. This thermal and tissue damage distribution in microwave-based therapies, especially in clinical applications like the ablation of deep tumors, is crucial. A precise understanding of the temperature pattern can help predict the effective treatment zone and prevent damage to surrounding healthy tissues.

Fig. 7 shows a region of tissue where the temperature has reached above 40°C.

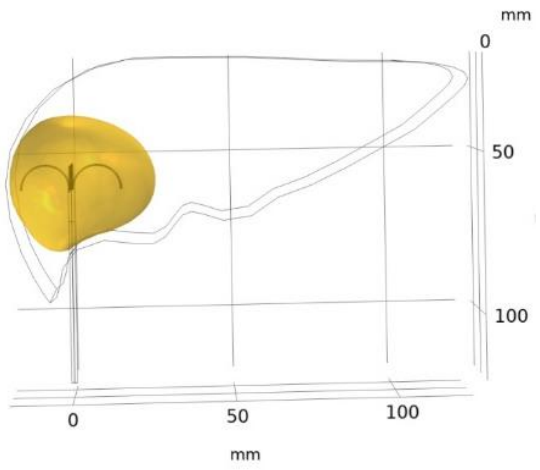

Fig. 7 Temperature contour in radiofrequency hyperthermia.

Within this range, complete tissue destruction (thermal necrosis) has occurred. In contrast, areas outside this range, where the temperature remains below 40°C, preserve healthy tissue, and no damage is observed. These observations are consistent with physiological and biophysical findings, as temperatures above 40–45°C are typically considered a critical threshold for the onset of protein denaturation and irreversible damage to cells. Therefore, precise control of temperature distribution during the thermal treatment process plays a key role in optimizing treatment effectiveness and preventing unintended damage to healthy tissues.

Fig. 8 displays the tissue necrosis changes over time during radiofrequency (RF) hyperthermia at various distances from the applicator, for two voltages of 22V and 17V. The x-axis represents the distance of different points from the trocar (the site where the applicator enters the tissue). in addition to examining the temperature distribution and the extent of necrosis in cancerous tissues, heat transfer to the surrounding healthy areas has also been addressed. These structures are highly sensitive to temperature elevations and are at risk of thermal damage, which can result in serious clinical complications and reduce the effectiveness of the treatment. Therefore, precise control of operational parameters such as input power and voltage, along with real-time monitoring of tissue temperature throughout the treatment process, is essential to prevent unintended damage to healthy tissues and to ensure patient safety. Based on diagrams 8-a and 8-b, it can be observed that in both cases, the closest point to the applicator reaches complete necrosis (necrosis value equal to 1) in less than one minute.

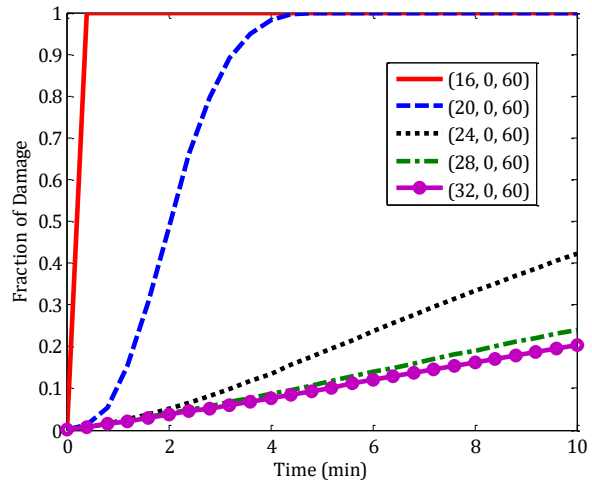

(a)

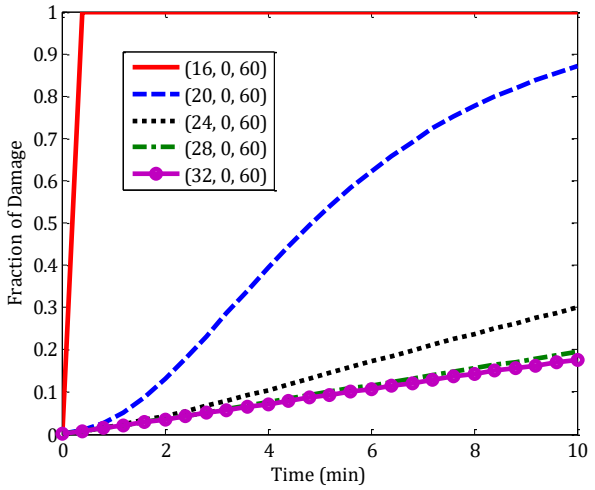

(b)

Fig. 8 Tissue necrosis as a function of time during radiofrequency hyperthermia at different distances from the applicator: (a) at 22V, (b) at 17V.

As the distance from the trocar increases, the degree of necrosis gradually decreases. This behavior is logical, as the intensity of the electric field and, consequently, the heat induced by radiofrequency waves is maximum near the applicator. As the distance from the heat source increases, both the field intensity and the heat decrease. The decrease in localized temperature results in less thermal damage to the tissue, leading to a lower degree of necrosis. Furthermore, an increase in voltage (22V compared to 17V) results in a higher field intensity and better heat distribution at greater distances from the

applicator, which contributes to more necrosis at farther distances.

Fig. 9 shows the changes in tissue necrosis over time during microwave treatment with input powers of 10W and 5W, and a fixed frequency of 2.45 GHz. Similar to the results in Fig. 8, it is observed that points close to the applicator reach complete necrosis in less than one minute.

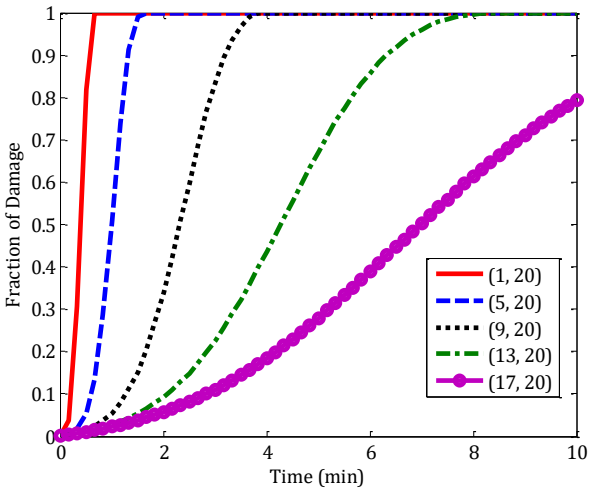

(a)

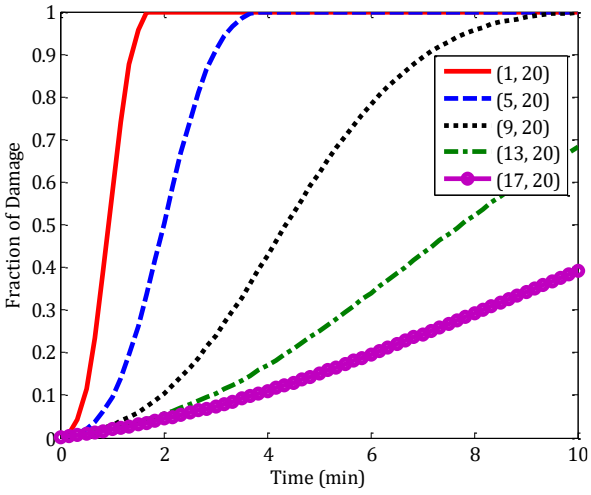

(b)

Fig. 9 Tissue necrosis as a function of time during microwave hyperthermia at different distances from the applicator: (a) at an input power of 10W and a frequency of 2.45 GHz, (b) at an input power of 5W and a frequency of 2.45 GHz.

As the distance from the applicator increases, the necrosis level continuously decreases, as in microwave hyperthermia, the energy absorption intensity is higher in regions closer to the antenna. Microwaves increase the temperature of surrounding tissues rapidly through dielectric heating. However, as the distance from the radiation source increases, energy loss (due to absorption, scattering, and reflection of the waves in the tissue) leads to a temperature drop, thereby reducing the intensity of necrosis. Additionally, increasing the input power from 5W to 10W results in a higher heat production rate, which causes a faster and more extensive tissue necrosis at greater distances.

Figs. 10 and 11 show the changes in tissue temperature at different locations relative to the applicator during the treatment process. In Fig. 10, which corresponds to microwave treatment, it can be seen from diagram 10-a that the closest point to the applicator reaches a temperature of about 100°C within 6 minutes. As the distance from the trocar increases, the tissue temperature decreases. This sharp temperature increase in the simulation, based on the actual geometry of the liver, appears unnatural and indicates excessive energy absorption in the area near the applicator. Therefore, it can be concluded that to prevent burns or uncontrolled severe tissue damage, the input power should be reduced so that the temperature increases only up to the necrosis threshold (45 to 60°C), avoiding the attainment of destructive high temperatures.

Fig. 11 shows the changes in tissue temperature near the applicator over time under different applied voltage conditions. In Fig. 11-a, hyperthermia is performed using radiofrequency waves at a voltage of 22V (based on previous report data and assuming a simplified liver geometry).

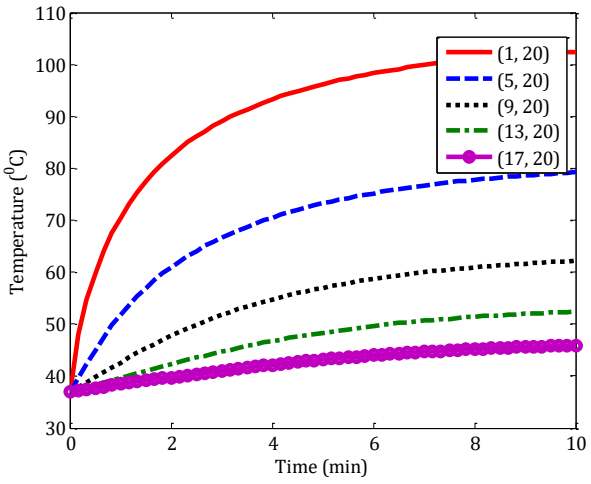

(a)

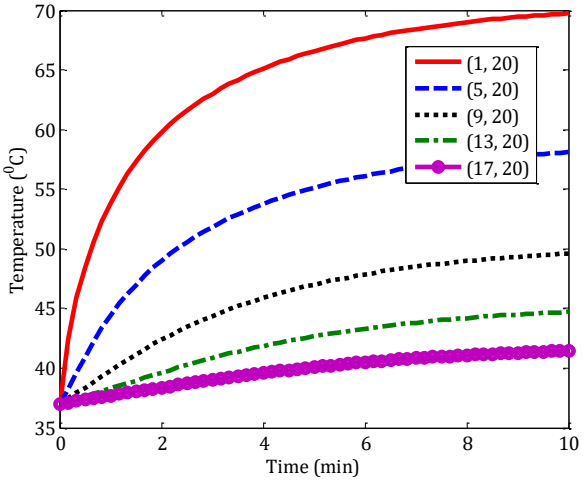

(b)

Fig. 10 Temperature as a function of time during microwave hyperthermia at different distances from the applicator: (a) at an input power of 10W and a frequency of 2.45 GHz, (b) at an input power of 5W and a frequency of 2.45 GHz.

The results indicate that the temperature at the closest point to the applicator reaches 380 Kelvin (approximately 107°C) within just 1 minute. This relatively high temperature and its unexpected increase suggest localized energy concentration in the complex structure of real tissue. Therefore, it can be concluded that to better control the temperature and prevent reaching excessively high temperatures that could lead to severe burns or uncontrolled tissue destruction, reducing the applied voltage from 22V to 17V is necessary. In Fig. 11-b, with the reduced applied voltage of 17V, the temperature at the closest point to the applicator reaches approximately 350 Kelvin (equivalent to 77°C) after 1 minute. This temperature is within the optimal range for thermal necrosis and significantly reduces the risk of severe damage to healthy tissues.

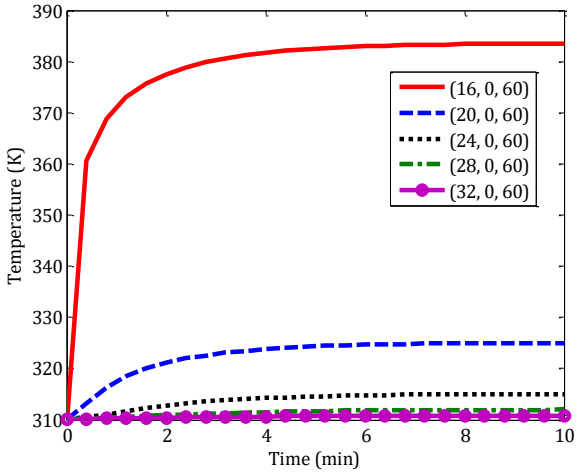

(a)

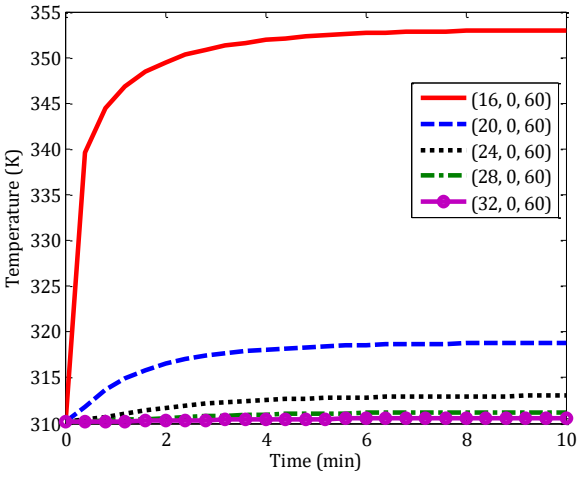

(b)

Fig. 11 Temperature as a function of time during radiofrequency hyperthermia at different distances from the applicator: (a) at 22V, (b) at 17V.

6-Conclusions

Microwave and radiofrequency hyperthermia are advanced and minimally invasive methods for cancer treatment, particularly for liver tumors. In this study,

the thermal and electrical effects of these waves on cancerous tissues were thoroughly investigated, demonstrating that heat distribution within the tissue is a key factor influencing the extent of cancer cell destruction and treatment success. Results showed that regions closest to the applicator experienced complete necrosis within a short time, while tissue temperature and necrosis gradually decreased with increasing distance. Moreover, simulations incorporating the liver's realistic geometry exhibited higher localized temperature elevations compared to simplified models, underscoring the importance of considering actual tissue structure.

However, clinical implementation of this method faces several challenges. Anatomical and physiological variations among patients can affect the accuracy of thermal predictions, precise temperature control in living tissues is complex, and there are potential risks such as unintended damage to healthy tissue. Additionally, extensive experimental studies and clinical trials are required to confirm the efficacy and safety of the technique.

Based on the findings, it is recommended to reduce the power to below 5 watts for microwaves and the voltage to approximately 17 volts for radiofrequency treatment to maintain temperature within the optimal necrosis range and prevent harm to healthy tissue. Overall, this study provides a foundation for optimizing non-invasive hyperthermia treatments and designing safer equipment; however, clinical application depends on addressing the mentioned challenges and limitations.

References

[1] Esmaeili, A., Hemami, R., Ghaffari, Y., & Abdollahi, S. (2022). A review on evaluation of natural polymers with the approach of drug delivery system using herbal plant microcapsules. *Journal of Simulation and Analysis of Novel Technologies in Mechanical Engineering*, *2*(2), 65.

[2] Ghorbani, A., Shahriari, S., & Gholami, A. M. (2021). Investigation of cell biomechanics and the effect of biomechanical stimuli on cancer and their characteristics. *Journal of Simulation and Analysis of Novel Technologies in Mechanical Engineering*, *13*(4), 67-79.

[3] Asgari, F., Minooei, A., Abdolahi, S., Shokrani Foroushani, R., & Ghorbani, A. (2021). A new approach using Machine Learning and Deep Learning for the prediction of cancer tumor. *Journal of Simulation and Analysis of Novel Technologies in Mechanical Engineering*, *13*(4), 41-51.

[4] Mohammad, N. D., Hassan, F., & Mina, T. (2013). Cancer metastasis, genetic and microenvironmental factors of distant tissue: a review article.

[5] Chiriac, H., Petreus, T., Carasevici, E., Labusca, L., Herea, D. D., Danceanu, C., & Lupu, N. (2015). In vitro cytotoxicity of Fe–Cr–Nb–B magnetic nanoparticles under high frequency electromagnetic field. *Journal of Magnetism and Magnetic Materials*, *380*, 13-19.

[6] Hervault, A., & Thanh, N. T. K. (2014). Magnetic nanoparticle-based therapeutic agents for thermo-chemotherapy treatment of cancer. *Nanoscale*, *6*(20), 11553-11573.

[7] Callstrom, M. R., & Kurup, A. N. (2009). Percutaneous ablation for bone and soft tissue metastases—why cryoablation?. *Skeletal radiology*, *38*, 835-839.

[8] Dodd, G. D., Soulen, M. C., Kane, R. A., Livraghi, T., Lees, W. R., Yamashita, Y., ... & Rhim, H. (2000). Minimally invasive treatment of malignant hepatic tumors: at the threshold of a major breakthrough. *Radiographics*, *20*(1), 9-27.

[9] Kuang, M., Lu, M. D., Xie, X. Y., Xu, H. X., Mo, L. Q., Liu, G. J., ... & Liang, J. Y. (2007). Liver cancer: increased microwave delivery to ablation zone with cooled-shaft antenna—experimental and clinical studies. *Radiology*, *242*(3), 914-924.

[10] Eslami, M., Mokhtarian, A., Pirmoradian, M., Seifzadeh, S. A., & Rafiaei, S. M. (2020). Designing and creating a virtual reality environment and a wearable glove with control and evaluation capability to rehabilitate patients.

[11] Paganini, A. M., Rotundo, A., Barchetti, L., & Lezoche, E. (2007). Cryosurgical ablation of hepatic colorectal metastases. *Surgical oncology*, *16*, 137-140.

[12] Berjano, E. J. (2006). Theoretical modeling for radiofrequency ablation: state-of-the-art and challenges for the future. *Biomedical engineering online*, *5*(1), 24.

[13] Haemmerich, D. (2010). Biophysics of radiofrequency ablation. *Critical Reviews™ in Biomedical Engineering*, *38*(1).

[14] Strohbehn, J. W. (1983). Temperature distributions from interstitial RF electrode hyperthermia systems: theoretical predictions. *International Journal of Radiation Oncology* Biology* Physics*, *9*(11), 1655-1667.

[15] Petryk, A. A., Giustini, A. J., Gottesman, R. E., Trembly, B. S., & Hoopes, P. J. (2013). Comparison of magnetic nanoparticle and microwave hyperthermia cancer treatment methodology and treatment effect in a rodent breast cancer model. *International Journal of Hyperthermia*, *29*(8), 819-827.

[16] Coughlin, C. T. (2023). Prospects for interstitial hyperthermia. In *Interstitial hyperthermia: physics, biology and clinical aspects* (pp. 1-10). CRC Press.

[17] Stigliano, R. V. (2014). *Development and validation of a treatment planning model for magnetic nanoparticle hyperthermia cancer therapy*. Dartmouth College.

[18] Qian, G. J., Wang, N., Shen, Q., Sheng, Y. H., Zhao, J. Q., Kuang, M., ... & Wu, M. C. (2012). Efficacy of microwave versus radiofrequency ablation for treatment of small hepatocellular carcinoma: experimental and clinical studies. *European radiology*, *22*, 1983-1990.

[19] Khokhlova, T. D., & Hwang, J. H. (2016). HIFU for palliative treatment of pancreatic cancer. *Therapeutic Ultrasound*, 83-95.

[20] Pillai, K., Akhter, J., Chua, T. C., Shehata, M., Alzahrani, N., Al-Alem, I., & Morris, D. L. (2015). Heat sink effect on tumor ablation characteristics as observed in monopolar radiofrequency, bipolar radiofrequency, and microwave, using ex vivo calf liver model. *Medicine*, *94*(9), e580.

[21] Lu, D. S., Raman, S. S., Vodopich, D. J., Wang, M., Sayre, J., & Lassman, C. (2002). Effect of vessel size on creation of hepatic radiofrequency lesions in pigs: assessment of the “heat sink” effect. *American Journal of Roentgenology*, *178*(1), 47-51.

[22] Yhamyindee, P., Phasukkit, P., Tungjitkusolmon, S., & Sanpanich, A. (2012, December). Analysis of heat sink effect in hepatic cancer treatment near arterial for microwave ablation by using finite element method. In *The 5th 2012 Biomedical Engineering International Conference* (pp. 1-5). IEEE.

[23] Ringe, K. I., Lutat, C., Rieder, C., Schenk, A., Wacker, F., & Raatschen, H. J. (2015). Experimental evaluation of the heat sink effect in hepatic microwave ablation. *PloS one*, *10*(7), e0134301.

[24] Ma, Z. H., Wang, Y. P., Zheng, W. H., Ma, J., Bai, X., Zhang, Y., ... & Hua, X. D. (2020). Prognostic factors and therapeutic effects of different treatment modalities for colorectal cancer liver metastases. *World Journal of Gastrointestinal Oncology*, *12*(10), 1177.

[25] Radmilović-Radjenović, M., Bošković, N., & Radjenović, B. (2022). Computational modeling of microwave tumor ablation. *Bioengineering*, *9*(11), 656.

[26] Gorman, J., Tan, W., & Abraham, J. (2022). Numerical simulation of microwave ablation in the human liver. *Processes*, *10*(2), 361.

[27] Liu, J., Gao, H., Wang, J., He, Y., Lu, X., Cheng, Z., & Wu, S. (2023). Recent research advances on simulation modeling of temperature distribution in microwave ablation of lung tumors. *Computer Assisted Surgery*, *28*(1), 2195078.

[28] Curley, S. A. (2003). Radiofrequency ablation of malignant liver tumors. *Annals of Surgical Oncology*, *10*, 338-347.

[29] Sazgarnia, A., Naghavi, N., Mehdizadeh, H., & Shahamat, Z. (2015). Investigation of thermal distribution for pulsed laser radiation in cancer treatment with nanoparticle-mediated hyperthermia. *Journal of thermal biology*, *47*, 32-41.

[30] SAWMPA, S. A. (2021). Three-dimensional numerical study for hepatic tumor ablation using electric current and bioheat transfer.

[31] Gorman, J., Tan, W., & Abraham, J. (2022). Numerical simulation of microwave ablation in the human liver. *Processes*, *10*(2), 361.

[32] Dahaghin, A., Emadiyanrazavi, S., Haghpanahi, M., Salimibani, M., Bahreinizad, H., Eivazzadeh-Keihan, R., & Maleki, A. (2021). A comparative study on the effects of increase in injection sites on the magnetic nanoparticles hyperthermia. *Journal of Drug Delivery Science and Technology*, *63*, 102542.

[33] Maaref, Y., Pakravan, H. A., & Jafarpur, K. (2019). Numerical Analysis of the Heat Sink Effect of Blood Vessels on Hepatic Radiofrequency and Microwave Ablation. *Modares Mechanical Engineering*, *19*(7), 1711-1720.